Empirical Relationships based on the P-wave Envelop for Distance and Magnitude Estimation for Earthquake Early Warning in Iran

Attieh Eshaghi[1], Mohammad P.M. Shahvar[1], Esmaeil Farzanegan[2], and Hossein Mirzaei Alavijeh[2]*

1. Assistant Professor, Road, Housing and Urban Development Research Center, Tehran, Iran,
* Corresponding Author; email: attieh.eshaghi@gmail.com
2. Faculty Member, Road, Housing and Urban Development Research Center, Tehran, Iran

Received: 07/10/2017
Accepted: 19/03/2018

ABSTRACT

The main goal of an Earthquake Early Warning (EEW) system is to reduce the damaging effects of the hazardous earthquakes. The characterization of an earthquake for EEW includes most importantly, the estimates of its size (magnitude) and location. In this study, the distance and magnitude of the selected earthquakes were estimated using the envelope of the initial part of the P-waveforms deploying a single seismic record. The method so called "B-delta" [1] is used to find the EEW parameters. In total, 1210 records (vertical component) with 4.0≤ M 7.7 and epicentral distance up to 300 km is used. The root mean square error (RMSE) of epicentral distance estimations using 2 and 3 sec P-wave time windows are 0.260 and 0.261 on a logarithmic scale respectively. Additionally, the C-Δ method [2] was performed to check if this method provides more accurate estimates. Results show no significant differences between the final estimates of the two methods. Furthermore, using the obtained epicentral distance, the magnitude was estimated by employing empirical magnitude-amplitude relationships. The magnitude RMSE of both methods is in range of 0.6-0.7. Results suggest that the final magnitude of the large events would be underestimated using just few seconds of P-wave; however, the magnitude estimates can be used as the minimum threshold for the final size of the ongoing event. Moreover, short term average/long term average method was used for automatic P-wave arrival detection. The result shows 76% success in P-wave arrival detection. This method can be utilized in real time EEW practices.

Keywords:
Earthquake Early Warning System; P-wave; B-delta method; Single Station method; Strong Motion Data; Iran

1. Introduction

Earthquake Early Warning (EEW) system's objective is to prevent and reduce the effects of hazardous earthquakes by providing a few to tens of seconds warning before the arrival of damaging ground motion to a specific location. In EEW applications, determination of the size and location of the ongoing earthquake is of the great importance [3]. During past decades, many researches have been conducted in order to estimate the EEW parameters rapidly after the P-wave detection (e.g. [4-6]). The first practical EEW system called "Urgent Earthquake Detection and Alarm System" (UrEDAS) [7-8] started its operation in Japan railways (JR) to stop Shinkansen high speed train. Later, in 2003, Odaka et al. [1] presented a new approach called "B-delta method" to estimate the epicentral distance and magnitude rapidly after the P-wave detection using a single recording [1, 9]. Their studies showed

a negative correlation between the initial rising slopes of the P-wave envelope of vertical ground motion records (B) and the epicentral distances (Δ) [1, 6, 9, 10]. In the so called 'B-Δ method', the function $Bt*exp(-At)$ is first fitted to the initial part of the P-wave envelope through the least square inversion, and then, the epicentral distance is estimated from the coefficient B. Afterward, the magnitude is estimated by employing a predefined attenuation relationship between magnitude, epicentral distance and the amplitude of initial P-wave. Currently, this method is in use by JR to control the Shinkansen high speed trains during the large earthquake [11-12]. As mentioned before, the epicentral distance and magnitude are determined from a single seismic record (on-site or single station method). Noda et al. [6] developed a new B-Δ relationship using new database. The final relation proposed in their study is as follows:

$$\begin{aligned} &log(\Delta) = -0.498\ log(B) + 1.965 \pm 0.32 \\ &tw = 2\ \text{sec} \end{aligned} \quad (1)$$

where B represents the growing slope of the initial P-wave envelope (Gal/s), Δ designates the epicentral distance (in kilometers) and 'tw' is the time window width of the analysis. The output of this method is also in use by Japan Meteorological Agency (JMA) that is responsible for providing tsunami forecasts and issuing EEW for upcoming strong motion since 2007 [13-14]. Iwata et al. [2] introduced a more simple fitting equation in order to improve the accuracy and speed of the P-wave warning, where the function $y(t) = C*t$ is fitted to the initial part of the P-wave envelop and the relation between C coefficient and epicentral distance was obtained. Their results showed 12% improvement in the accuracy of epicentral estimations using C-Δ approach in comparison to the B-Δ approach. It should be mentioned that, the EEW parameters are updated as more data become available. When the number of stations that are recording the earthquake is increased, other approaches such as the so called "Territory method" or the "Grid search method" [15] are used to calculate the hypocenter location and magnitude of the event (network based approach).

Iran is one of the most active seismic zones in the world, which has experienced many destructive earthquakes during its long history. Most of the Iran's major cities, such as Tehran, Tabriz and Shiraz are exposed to earthquake hazards. Recently, there have been some ongoing projects for implementation and application of the EEW and rapid response systems in major cities of Iran. For example, Building and Housing Research Center (BHRC) has initiated a project for rapid response system for earthquake in Tehran. Besides, Tehran Disaster Mitigation and Management Organization (TDMMO) in collaboration with Japan International Cooperation Agency (JICA) started a pilot project for EEW system in Tehran [16]. Heidari [16] used 440 vertical acceleration waveforms from 17 earthquakes (2003-2014) to investigate the distance and magnitude scaling relationships using the B-Δ method. He presented Equation (2) for two sec of the P-wave window as one of his final relations:

$$\begin{aligned} &log(\Delta) = -0.908\ log(B) + 2.527 \pm 0.17 \\ &tw = 2\ \text{sec} \end{aligned} \quad (2)$$

The observed slope of the final epicentral distance- B relation is clearly lower than the one for Japan (see Equation 1), which is argued to be the consequence of the tectonic difference of the two regions [16]. In another study, Mahood et al. [17], performed B-delta method for a case study of Ahar-Varzaghan earthquake. They used 48 vertical-component accelerograms of the Ahar-Varzaghan earthquake (with Mw 4.5-6.4 and epicentral distances <100 km) to calculate the magnitude and distance of the Ahar-Varzaghan earthquake.

In this study, a more complete database (1996-2016) from BHRC data bank (see Data and Resources) was collected, and both B-Δ and C-Δ approaches were performed to find the best relationship to estimate the epicentral distance and magnitude of the earthquakes for EEW applications in Iran. Furthermore, for the P-wave detection, the Short Term average/Long Term average (STA/LTA) method was tested [18-19], which monitors the average energy in a short term average leading window, to the long term average window with the same parameters as presented in RTRI report, 20013 [19]. The proper P-wave detection has an important role when the seismic parameters are estimated based on the initial part of the P-waveforms for EEW purposes.

2. Strong Ground Motion Data and Processing

In this study, recordings from 349 earthquakes with $M \geq 4.0$ from 1966 - 2016 with focal depth ≤ 70 km and epicentral distance of up to 300 km were analyzed (Table 1), recorded by Iran Strong Motion Network (ISMN) stations at BHRC (see Data and Resources). Figure (1) shows the map of the selected earthquakes along with the BHRC recording stations. The preferred moment magnitude (M) of each event was selected from the Global Centroid Moment Tensor (CMT) catalog (see Data and Resources) and BHRC catalog respectively (for those events that M was not reported in CMT catalog, the BHRC moment magnitude was accepted). Figure (2) shows the distribution of the focal depth and epicentral distance versus moment magnitude for the whole database. Generally, there are more records for $M < 7$ with distances up to 100 km. In processing of the data, first, all records (in total 2690 vertical records) were checked visually for the data quality and clear P-wave arrival, and then recordings with clear P-wave arrival that have at least few sec of pre-event window were accepted. The P-wave onset for each recording is manually picked (Figure 3). Afterward, all recordings were filtered using a band-pass Butterworth filter with an order of 4 and corner frequencies that were selected using the signal to noise (S/N) ratio (the bandwidth was selected that the S/N ratio was ≥ 3.0).

Table 1. Data used in this study.

Year	Number of Earthquakes	Depth	Epicentral Distance	Magnitude
1996-2016	349	≤70 km	0-300 km	4-7.7

2.1. P-wave Detection

In real time EEW practices when the EEW parameters are estimated based on the initial P-wave information, the correct P-wave detection has a significant effect on the final results. Currently, most of the seismic instruments use the STA/LTA method for the automatic P-wave detection [2, 18]. In order to pick the P-wave arrival automatically for EEW performance in real time and to check the accuracy of the P-wave arrival detection with this method,

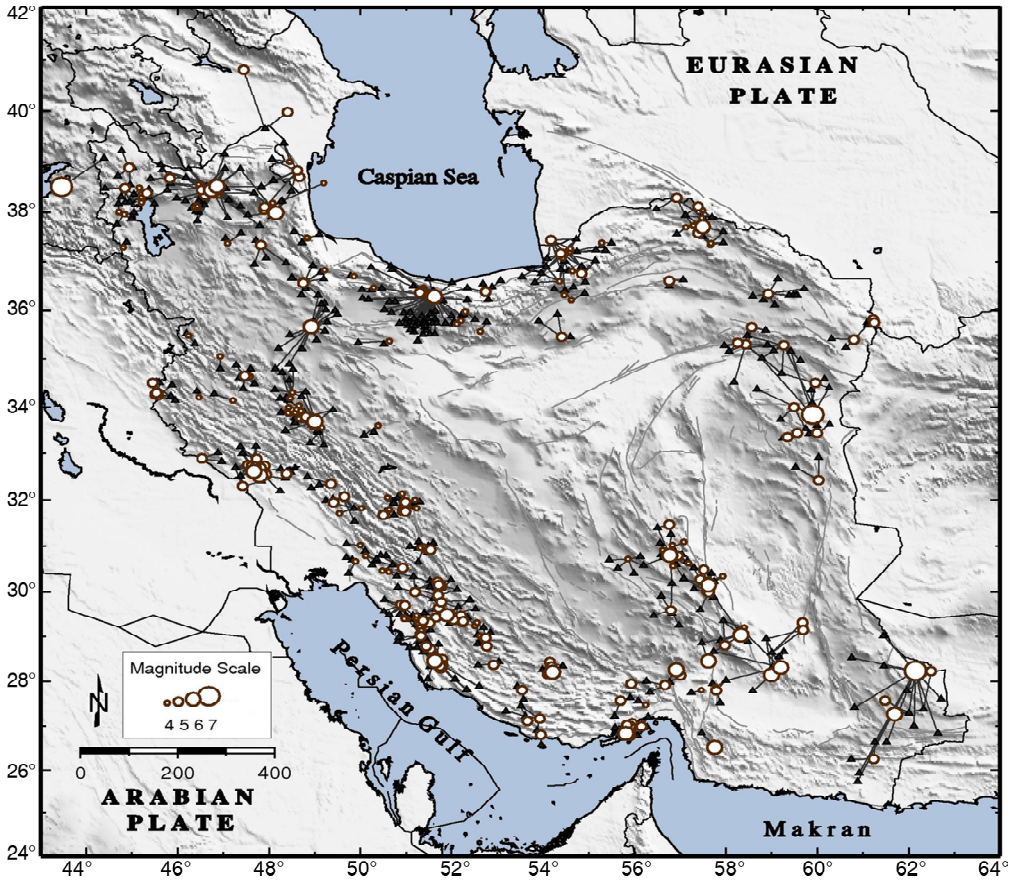

Figure 1. Spatial distribution of the selected earthquakes used in this study along with the recording ISMN stations (gray triangles). Different symbols show the magnitude range of the selected earthquakes.

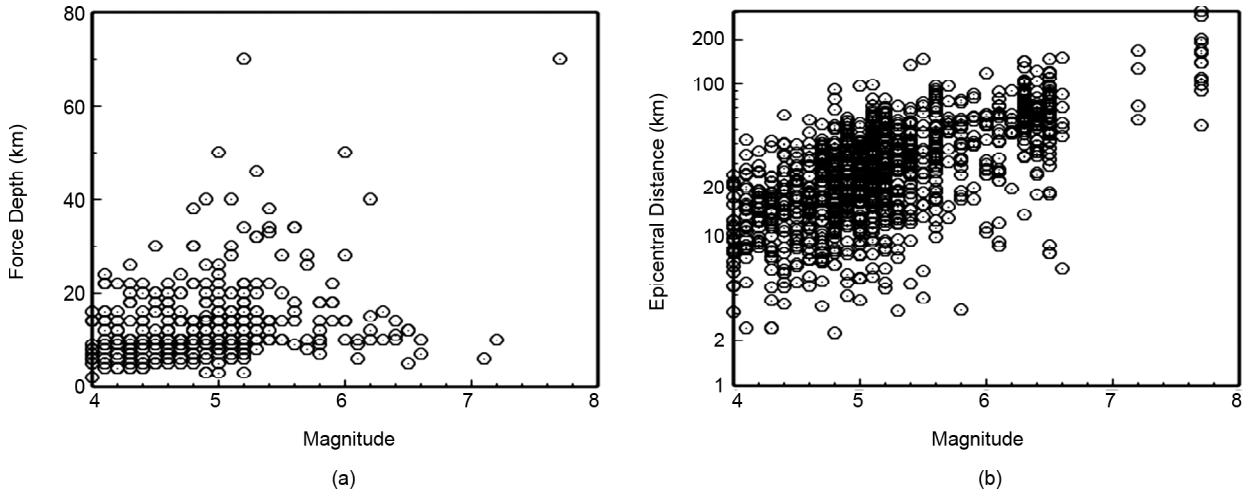

Figure 2. (a) Focal depth-magnitude distribution and (b) epicentral distance-magnitude distribution for the dataset used in this study.

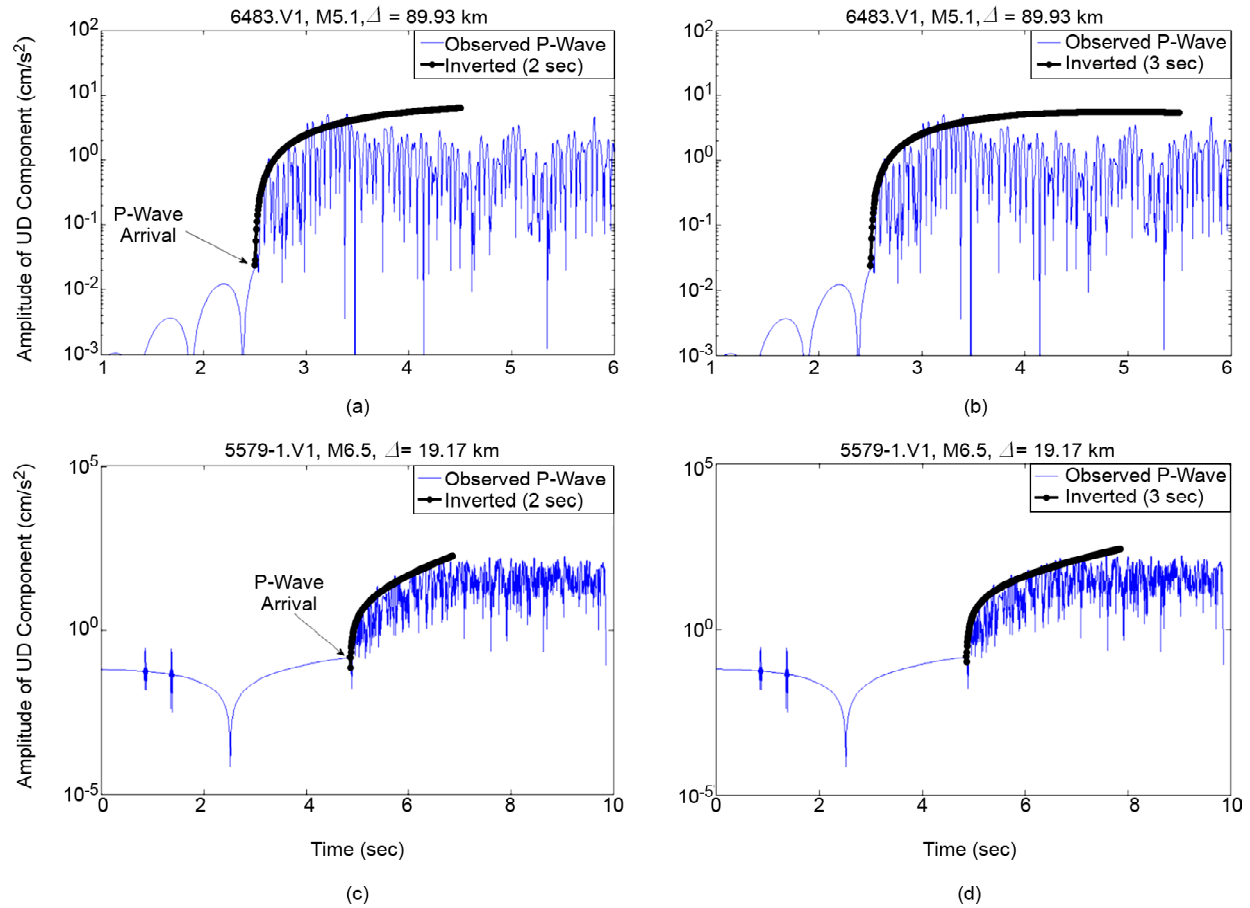

Figure 3. Logarithmic P-waveform samples of two earthquakes at two different epicentral distances (Δ) for 2 sec (a, c) and 3 sec of P-wave (b, d). Top row is related to a M5.1 earthquake at 89.93 km distance (a, b) and the bottom one is for a M6.5 earthquake at 19.17 km distance (c, d).

here in this study, the STA/LTA method was tested with proposed parameters of $\alpha_n = 0.9999$ and $\alpha_u = 0.96$ [19]. This analysis showed that this technique picked the P-wave arrival correctly in 76% of the recordings. The Amplitude of the short term and long term averaged windows were defined as the following equations, respectively:

$$UD(s) = (1-) * ud(s) + \alpha_u * UD(s-1) \quad (3)$$

$$NL(s) = (1-) * ud(s) + \alpha_n * NL(s-1) \quad (4)$$

where *UD* is the amplitude level, *ud* is the vertical acceleration, *s* is the sample number, *NL* is the noise level, and α_u and α_n are the smoothing coefficients. This method certainly increases the

accuracy of automatic P-wave detection during the large earthquakes, which is a vital task for real time EEW practices.

3. Seismic Parameter Estimation

Previous studies (e.g. [1, 9, 11]) showed that the B-Δ method provides an empirical relation between epicentral distance and the growth rate of the initial P-waveform envelop (coefficient B). Here, the coefficients A and B were determined by fitting Equation (5) to the observed P-wave envelope of the vertical components of the recorded accelerograms (for 2 and 3 sec windows) through the least squares inversion.

$$y(t) = Bt * exp(-At) \quad (5)$$

To do this, following Odaka et al. [1], first, the logarithm of the absolute values of the waveforms was calculated; then, the P-wave envelop was constructed by keeping the maximum value of the acceleration in each time step. The P-wave arrival time is taken as the origin time. As previously explained, *B* coefficient represents the slope of the initial part of the P-wave (or the rate of the P-wave growth), which is mainly dependent on distance, and *A* coefficient is related to the amplitude variation with time [1]. Some examples of the observed P-waveforms (solid lines) along with the fitting curves (dotted lines) for two time windows (2 and 3 sec) are shown in Figure (3). Iwata et al. [2] proposed a simplified equation (Equation 6), which shortened the length of data calculation. They argued that this simplified equation improved both the speed and accuracy of the results, which are important factors in EEW applications. Following Iwata et al. [2], we also fitted Equation (6) to the initial P-wave envelop and determined the *C* coefficient using the least square inversion.

$$y(t) = C * t \quad (6)$$

Figure (4) shows the relationships between coefficients B and C with the epicentral distances. There are clear linear relations between epicentral distances with coefficients B and C in logarithm scale; however, the scatter on the resulting values is somehow high. The obtained B values of two time

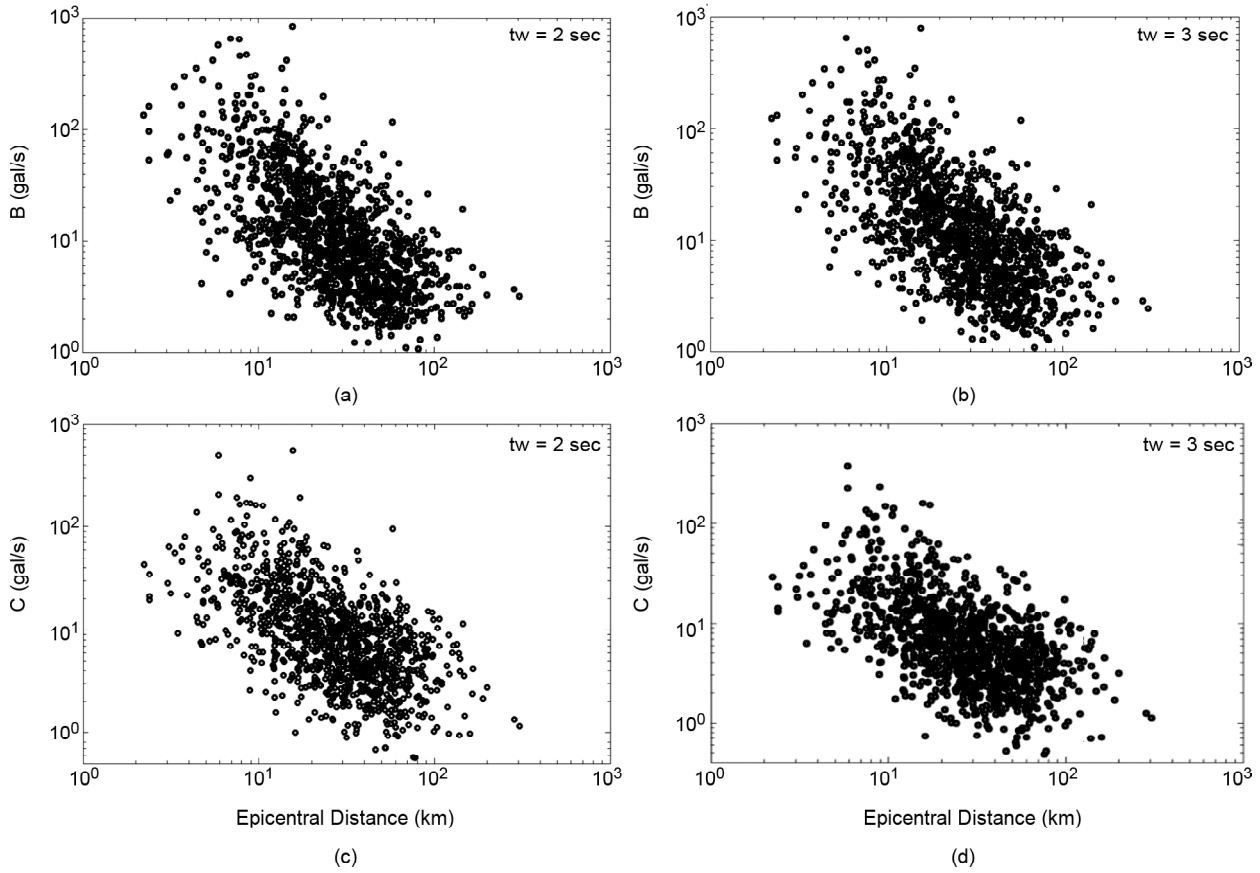

Figure 4. B values (a, b) and C values (c, d) versus epicentral distance for earthquakes used in this study. The time window width of the analysis is shown by 'tw'.

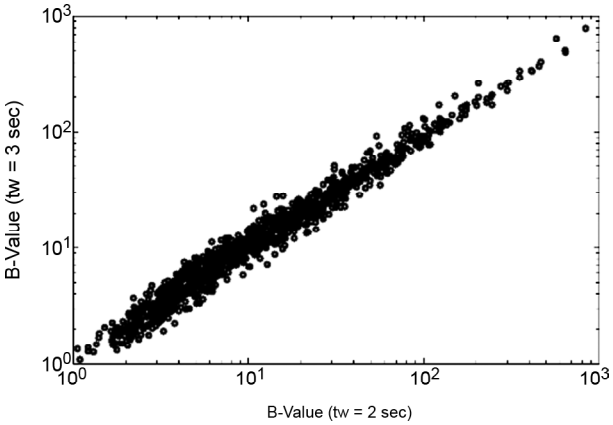

Figure 5. log B values for 2 and 3 sec time-window widths (using Equations 7 and 8). There is a strong correlation between these two values.

window widths (2 and 3 sec) are compared in Figure (5). As it can be seen, there is a strong correlation between these two values. The empirical relationship between $log\Delta$ with $logB$ and $logC$ are determined as the following equations for two different time windows (2 and 3 sec):

$$log(\Delta) = -0.419 log(B) + 1.865 \pm 0.260 \quad tw = 2\ sec \tag{7}$$

$$log(\Delta) = -0.426 log(B) + 1.875 \pm 0.261 \quad tw = 3\ sec \tag{8}$$

$$log(\Delta) = -0.422 log(B) + 1.811 \pm 0.274 \quad tw = 2\ sec \tag{9}$$

$$log(\Delta) = -0.420 log(B) + 1.760 \pm 0.281 \quad tw = 3\ sec \tag{10}$$

To calculate the root mean square error (RMSE), the difference between $log10(\Delta_{observed})$ and $log10(\Delta_{predicted})$ were calculated. The resulted RMSE shows that the C-Δ approach does not make a significant difference on the final epicentral distance results in comparison to the B-Δ method. Somehow, all equations have similar RMSE values. Another interesting observation is that the calculated slope and the constant values here in this study are more similar to the results presented by Noda et al. [6] (compare Equations 1 and 7) which is completely different from the results by Heidari [16].

4. Magnitude Estimation

After determining the epicentral distance, similar to Odaka et al. [1], the magnitude is estimated via:

$$\boldsymbol{M} = a\ log\ A_{max} + b\ log\ (para) + c \tag{11}$$

where $\boldsymbol{M}$ is the moment magnitude, A_{max} is the maximum vertical acceleration amplitude of the P-waves within the specified time interval, para is either B or C coefficient, and the unknown coefficients a, b and c are determined through the least square method. The following equations were determined using B and C parameters:

$$\boldsymbol{M} = 0.676 log(A_{max}) - 1.062 log(B) + 5.588 \pm 0.632 \quad tw = 2\ sec \tag{12}$$

$$\boldsymbol{M} = 0.917 log(A_{max}) - 1.224 log(B) + 5.430 \pm 0.615 \quad tw = 3\ sec \tag{13}$$

$$\boldsymbol{M} = 1.419 log(A_{max}) - 1.677 log(B) + 5.22 \pm 0.684 \quad tw = 2\ sec \tag{14}$$

$$\boldsymbol{M} = 1.980 log(A_{max}) - 2.146 log(B) + 4.578 \pm 0.698 \quad tw = 3\ sec \tag{15}$$

After determination of the unknown parameters, in case of the occurrence of a new earthquake, the epicentral distance is estimated by Equations (7) to (10), and then, the magnitude can be estimated based on Equations (12) to (15). The relationships between B and Amax in logarithmic space for 2 and 3 sec time windows for all the dataset is shown in Figure (6). There is a linear relationship between $log(B)$ and $log(A_{max})$. Figure (7) shows the histograms of epicentral distance residuals using B-Δ and C-Δ approaches. It can be seen that the distribution of the residuals are similar for both approaches, where they have similar ranges of RMSE values; however, the smallest RMSE is related to the B-Δ method for 2 sec of P-wave window ($\sigma = 0.260$). The histograms of magnitude residuals are shown in Figure (8). As it can be seen, the RMSE of magnitude does not decrease significantly when C-Δ approach is used, and the smallest RMSE belongs to B-Δ relation for 3 sec of P-wave time window. Besides, the use of maximum displacement amplitude (d_{max}) was tested instead of A_{max} in Equation (11). The resulted equations are as follows:

$$\boldsymbol{M} = 0.776 log(d_{max}) - 1.092 log(B) + 6.250 \pm 0.625 \quad t_w = 2\ sec \tag{16}$$

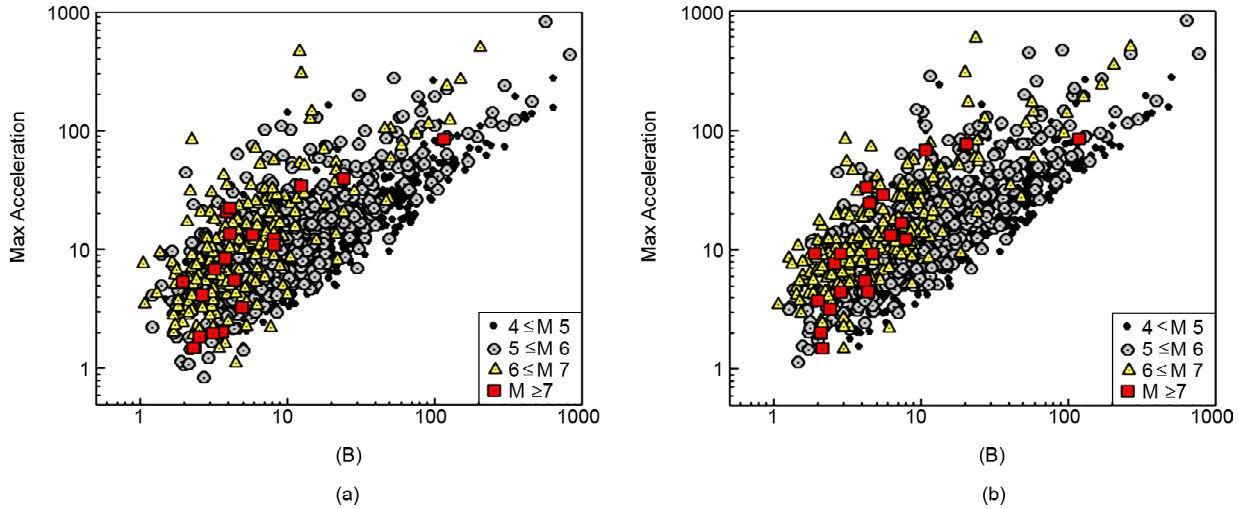

Figure 6. Maximum vertical accelerations values versus B-values for (a) 2 sec and (b) 3 sec of the P-waveforms. Different symbols show the range of magnitudes. The linear relationship can be seen between maximum accelerations and B-values for the initial P-waveforms time window.

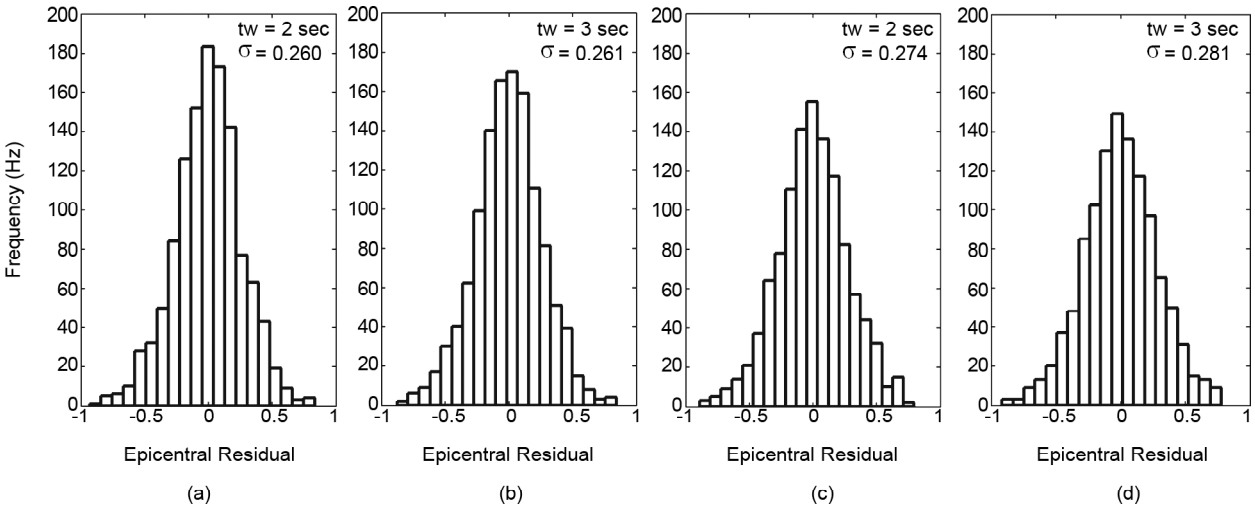

Figure 7. Histograms of the epicentral distance residuals ($\log10(\Delta_{observed})$ - $\log10(\Delta_{predicted})$) based on B-$\Delta$ approach (a, b) and C-Δ approach (c, d) for all dataset. σ represents the RMS of the epicentral distances residuals.

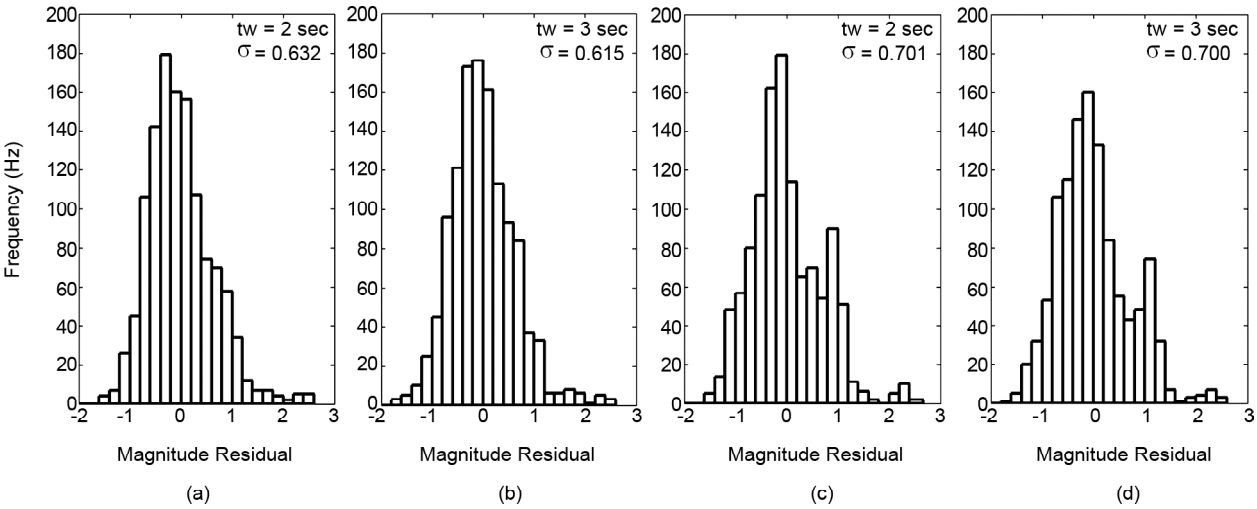

Figure 8. Histograms of the magnitude residuals ($M_{reported}$-$M_{estimated}$) based on Equation (11) for B-Δ (a, b) and C-Δ (c, d) approaches for all dataset. σ represents the RMS of the magnitude residuals.

$$\boldsymbol{M} = 1.038log\left(d_{max}\right) - 1.222log\left(B\right) + 5.947 \pm 0.600 \qquad t_w = 3\ sec \tag{17}$$

$$\boldsymbol{M} = 0.346log\left(d_{max}\right) - 0.635log\left(B\right) + 5.798 \pm 0.701 \qquad t_w = 2\ sec \tag{18}$$

$$\boldsymbol{M} = 0.987log\left(d_{max}\right) - 1.087log\left(B\right) + 5.516 \pm 0.700 \qquad t_w = 3\ sec \tag{19}$$

The RMSE of the magnitude estimation is reduced but not significantly, and because the acceleration amplitudes are faster to estimate, it is faster to use the acceleration amplitude for magnitude estimation in EEW applications. The presented magnitude scaling relationships (Equations 12-19) are linear relationships that can be used for magnitude estimation. However, in 2015, Iwata et al. [2] showed that adding an internal damping member would increase the accuracy of the magnitude estimations (Equation 20). The following equation was also tested here:

$$\boldsymbol{M} = a1\,log\,A_{max} + b1\,log\left(\Delta_{para}\right) + c1 + d1\left(\Delta_{para}\right) \tag{20}$$

where Δ_{para} is the estimated epicentral distance based on either *B*-Δ or *C*-Δ approaches and *a*1 to *d*1 are the unknown parameters that are determined using the least square method. The following equations were obtained for our database using Equation (20):

$$\boldsymbol{M} = 0.642log\left(A_{max}\right) - 14.55log\left(\Delta_B\right) - 3.7178 + 7.2903\left(\Delta_B\right) \pm 0.621 \qquad tw = 2\,sec \tag{21}$$

$$\boldsymbol{M} = 0.882log\left(A_{max}\right) - 14.577log\left(\Delta_B\right) - 4.4742 + 7.592\left(\Delta_B\right) \pm 0.603 \qquad tw = 3\,sec \tag{22}$$

$$\boldsymbol{M} = 1.362log\left(A_{max}\right) - 14.090log\left(\Delta_C\right) - 6.0726 + 8.370\left(\Delta_C\right) \pm 0.677 \qquad tw = 2\,sec \tag{23}$$

$$\boldsymbol{M} = 1.9321log\left(A_{max}\right) - 12.128log\left(\Delta_C\right) - 7.950 + 8.907\left(\Delta_C\right) \pm 0.693 \qquad tw = 3\,sec \tag{24}$$

Equations (21) to (24) indicate that the RMSE of magnitude estimations are slightly reduced when Equation (20) is used instead of Equation (11). The histograms of magnitude residuals based on Equation (20) are shown in Figure (9). One important point here is that the highest magnitude residual ($\boldsymbol{M}_{reported}$ - $\boldsymbol{M}_{estimated}$) is related to the largest magnitude (*M*7.7) in our database (Figure 10). Note that the records of this earthquake have rather large epicentral distances. We do not have other very large events (i.e. $M > 7.5$) in close distances in our database, which makes it more difficult to judge the performance of these P-wave methods for large events in close distances. However, the distribution of residual versus epicentral distance in Figure (10) suggests that the few seconds of P-wave underestimates the magnitude of large events, especially in larger distances. The distribution of magnitude residuals versus epicentral distance obtained using all other empirical magnitude-distance equations (Equations 12-24) follow the same behavior as is shown in Figure (10). Generally, *B*-Δ and *C*-Δ relations underestimate the magnitude of very large

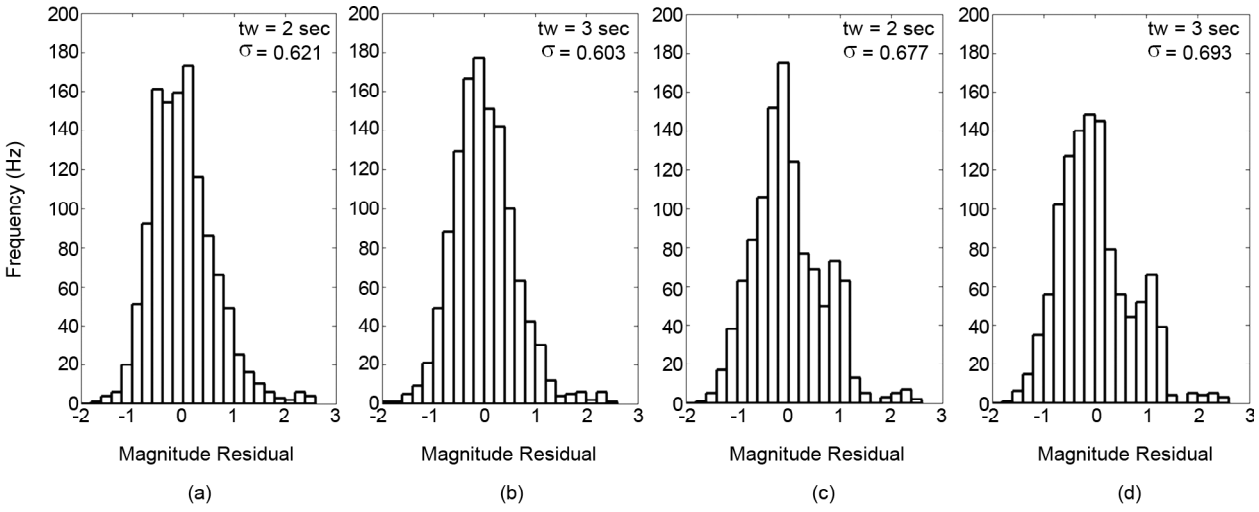

Figure 9. Histograms of the magnitude residuals ($M_{reported}$-$M_{estimated}$) based on Equation (20) for B-Δ (a, b) and C-Δ (c, d) approaches for all dataset. σ represents the RMS of the magnitude residuals.

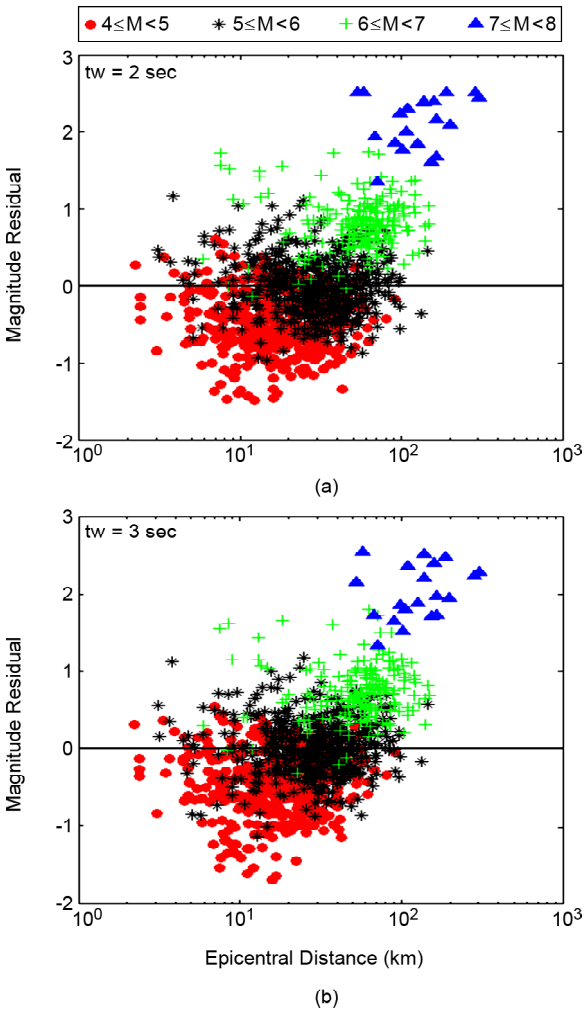

Figure 10. Distribution of magnitude residuals ($M_{reported}$ - $M_{estimated}$) versus epicentral distance for 2 sec (a) and 3 sec (b) of the P-wave using B-delta method (Equations 12 and 13).

events, which is not unexpected, because just 2 or 3 sec of the P-wave data is used. Previous studies about the seismic rupture confirmed that the determination of the final size of the large earthquakes within the few initial seconds of the P-waveforms is physically very obscure, where the major rupture lasts for several seconds to several tens of seconds [20-21]. Here, our analysis reveals the same results, where using a few seconds of initial P-wave would not determine the final size of a very large event accurately (Figure 10). However, the output of the *B*-Δ and *C*-Δ relations provide the preliminary estimates that can be used as the minimum threshold of the final size of the event, and depending on how close the earthquake is, some actions can be taken to reduce the hazardous effects of earthquakes. As previously mentioned, when more data become available, other EEW methods should be used to provide more accurate estimates with lower uncertainty. The results of the *B*-Δ and *C*-Δ approaches in *JR* practices show the successful outcome of these approaches, especially for large earthquakes such as 2011 *M*9.0 Tohoku event, where all trains were stopped before the strong shaking reach them and there were no casualties because of train derailment [20, 22]. Although the magnitude of Tohoku event was underestimated, the warning sent out earlier than the severe shaking [11, 20, 22]. For such applications, the scaling relationships presented in this study are very fundamental.

5. Discussion and Conclusions

In this study, the empirical magnitude and epicentral distance scaling relationships were developed to rapidly estimate the epicentral distance and magnitude of an earthquake for single station EEW applications in Iran. Here, good quality acceleration waveforms of earthquakes between 1996 and 2016 with $M \geq 4.0$ from BHRC data bank were collected. Following Odaka et al. [1] and Iwata et al. [2], in this study both *B*-Δ and *C*-Δ approaches were performed to find the magnitude and epicentral distance scaling relationships. We found the same observation, where the epicentral distance (Δ) and the rising slope of amplitude at its initial part (*B* or *C* coefficient) have linear relationships (see Figure 4).

Figure (11) shows the relationship between observed epicentral distance and the *B* values for 2

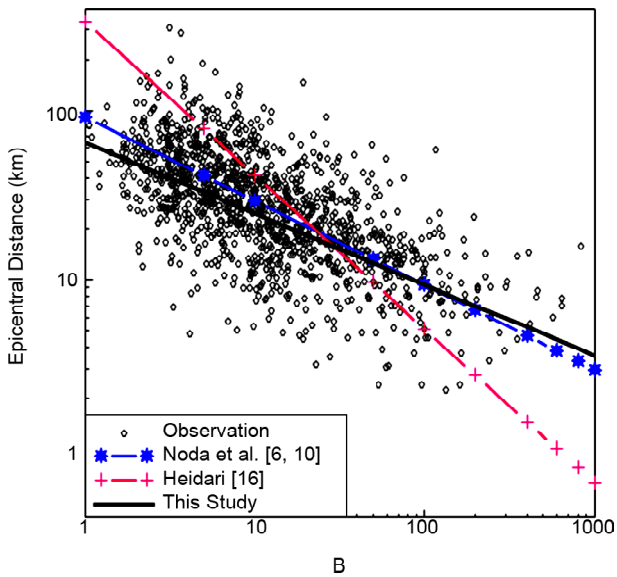

Figure 11. Relationships between epicentral distance and the obtained B values of the studied earthquakes along with the equations reported by other studies (as shown in the figure legend).

sec of the P-wave data for Iran's earthquakes along with the reported scaling relationships by Heidari [16] and Nodat et al. [6]. As it can be seen from Figure (11), the obtained scaling relationship here in this study is very close to the relation presented for Japan [6]. It can be argued that the relation between the growth rate of the P-wave and the distance is rather independent of the region. The scaling relationship reported by Heidari [16] is completely different (Figure 11) and it is suggested that TDMMO re-evaluate the empirical relationships for the EEW practices in Iran.

The resulted RMSE of epicentral distances and magnitudes for both B-Δ and C-Δ approaches are in similar ranges. The smallest RMSE of epicentral distance estimates is related to the B-Δ relation using 2 sec of P-waveforms (Equation 5), which is 0.260 for $log10(\Delta)$. Although the scatter of the data is rather high, considering the quite short time widths of the analysis (2 or 3 sec), the results would be acceptable. The largest observed magnitude residual is related to the largest event (M7.7), confirming that methods that use the initial P-waveforms would underestimate the final size of the large event (Figure 10); however, they enable us to provide a minimum threshold for the final size of the ongoing event that is a vital task for EEW practices. The obtained magnitude estimation results suggest that when more data become available, other EEW approaches, especially the network based methods, should be used to estimate the final size of the ongoing event.

Moreover, the STA/LTA method was tested for automatic P-wave arrival detection with the same parameters as proposed by RTRI report [19]. The results showed that in 76% of the total recording, this method could detect the P-wave arrival properly. Implementation of this method will increase the accuracy of the P-wave arrival detection for real time EEW applications.

6. Data and Resources

Strong ground motion data used in this study were collected from Iran Strong Motion Network (http://ismn.bhrc.ac.ir/, last accessed May 2016) of the Road, Housing & Urban Development Research Center (BHRC). The preferred assigned moment magnitude (M) for each event is that reported by the Global Centroid Moment Tensor (CMT) catalog (http://www.globalcmt.org/, last accessed May 2016) and BHRC catalogue respectively. Matlab was used for parameter estimations. All graphics were produced either using CoPlot software (www.cohort.com; last accessed May 2017) or Matlab.

References

1. Odaka, T., Ashiya, K., Tsukada, S., Sato, S., Ohtake, K., and Nozaka, D. (2003) A new method of quickly estimating epicentral distance and magnitude from a single station record. *Bull. Seismol. Soc. Am.*, **93**(1), 526-532.

2. Iwata, N., Yamamoto, S., Korenaga, M., and Noda, S. (2015) Improved algorithms of seismic parameter estimations and noise discrimination in earthquake early warning. *Quarterly Report of RTRI*, **56**(4), 291-298.

3. Allen, R.M. and Kanamori, H. (2003) The potential for earthquake early warning in southern California. *Science*, **300**(5620), 786-789.

4. Wu, Y.M., and Kanamori, H. (2005) Experiment on an onsite early warning method for the Taiwan early warning system. *Bull. Seismol. Soc. Am.*, **95**(1), 347-353.

5. Allen, R.M., Gasparini, P., Kamigaichi, O., and Bose, M. (2009) The status of earthquake early warning around the world: An introductory overview. *Seismological Research Letters*, **81**(5), 682-693.

6. Noda, S., Yamamoto, S., and Sato, S. (2012b) New method for estimating earthquake parameters for earthquake early warning. *Quarterly Report of RTRI*, **53**(2), 112-116.

7. Bito, Y. and Nakamura, Y. (1986) *Urgent Earthquake Detection and Alarm System*. Civil Engineering in Japan, Japan Society of Civil Engineers, Tokyo, Japan, 103-116.

8. Nakamura, Y. (1988) On the urgent earthquake detection and alarm system (UrEDAS). *Proc. of Ninth World Conference on Earthquake Engineering*, Tokyo, Japan, (**VII**), 673-678.

9. Odaka, T., Nakamura, H., and Ashiya, K. (2005) Difference in the initial slopes of the P-wave

envelope waveforms of the main shock *M*7.4 and foreshock M7.1 of the 2004 off the Kii peninsula earthquakes. *Earth, Planets and Space*, **57**(4), 333-337.

10. Noda, S., Yamamoto, S., Sato, S., Iwata, N., Korenaga, M., and Ashiya, K. (2012a) Improvement of back-azimuth estimation in real-time by using a single station record. *Earth, Planets and Space*, **64**(3), 315-318.
11. Yamamoto, S. and Tomori, M. (2013) Earthquake early warning system for railways and its performance. *Journal of JSCE*, **1**, 322-328.
12. Yamamoto, S., Iwata, N., Noda, S., and Korenaga, M. (2015) Improvement of the single-station EEW algorithms for railways. *Japan Geoscience Union Meeting*.
13. Kamigaichi, O., Saito, M., Doi, K., Matsumori, T., Tsukada, S., Takeda, K., Himoyama, T., Nakamura, K., Kiyomoto, M., and Watanabe, Y. (2009) Earthquake early warning in Japan: warning the general public and future prospects. *Seismol. Res. Lett.*, **80**, 717-726.
14. Doi, K. (2011) The operation and performance of earthquake early warnings by the Japan meteorological agency. *Soil Dynam. Earthq. Eng.*, **31**, 119-126, doi: 10.1016/j.soildyn.2010.06.009.
15. Horiuchi, S., Negishi, H., Abe, K., Kamimura, A., and Fujiwara, Y. (2005) An automatic processing system for broadcasting earthquake alarms. *Bull. Seismol. Soc. Am.*, **95**(2), 708-718.
16. Heidari, H. (2016) Quick estimation of the magnitude and epicentral distance using the P wave for earthquakes in Iran. *Bull. Seismol. Soc. Am.*, **106**(1), 225-231, doi: 10.1785/0120150090.
17. Mahood, M., Mokhtari, M., and Zafarani, H. (2016) Prediction of magnitude and epicentral distance from a single seismic record: A case study of the Ahar-Varzaghan earthquake. *International Journal of Geohazards and Environment*, **2**(4), 208-213.
18. Allen, R.V. (1978) Automatic earthquake recognition and timing from single traces. *Bull. Seismol. Soc. Am.*, **68**(5), 1521-1532.
19. Railway Technical Research Institute (RTRI) (2016) Annual report 2012-2013, P. 11. (http://www.rtri.or.jp/ last accessed 2016).
20. Hoshiba, Y., Iwakiri, K., Hayashimoto, N., Shimoyama, T., Hirano, K., Yamada, Y., Ishigaki, Y., and Kikuta, H. (2011) Outline of the 2011 off the pacific coast of Tohoku earthquake (*M* 9.0) earthquake early warning and observed seismic intensity. *Earth, Planets and Space*, **63**, 547-551.
21. Yamamoto, S., Sato, S., Iwata, N., Korenaga, M., Ito, Y., and Noda, S. (2011) Improvement of seismic parameter estimation for the earthquake early warning system. *Quart. Rep. RTRI*, **52**(4), 206-209, CrossRef (http://dx.doi.org/10.2219/rtriqr.52.206).
22. Japan Meteorological Agency (2011) Retrieved from http://www.seisvol.kishou.go.jp/eq/EEW/kaisetsu/joho/20110311144640/content/content_out.html, last accessed July, 2013.